

Eutectic Structures Competition in the Stripes Strengthening the (Zn) – Single Crystal

W. Wołczyński^{a,*}, S. Kjelstrup^b, D. Bedeaux^b, J. Szajnar^c, B. Billia^d

^aInstitute of Metallurgy and Materials Science, Polish Academy of Sciences, 30-059 Kraków, Reymonta 25, Poland

^bDepartment of Chemistry, Norwegian University of Science and Technology, 7491 Trondheim, Norway

^cDepartment of Foundry Engineering, Silesian University of Technology, Towarowa 7, 44-100 Gliwice, Poland

^dFaculte des Sciences et Techniques, Universite d'Aix-Marseille,
13397 Marseille, Av.Escadrille Normandie-Niemen, France

*Corresponding author. E-mail address: w.wolczynski@imim.pl

Received 4.04.2014; accepted in revised form 15.07.2014

Abstract

Some eutectic stripes have been generated in a hexagonal (Zn) - single crystal. The stripes are situated periodically with the constant inter-stripes spacing. The eutectic structure in the stripes consists of strengthening inter-metallic compound, $Zn_{16}Ti$, and (Zn) – solid solution. The rod-like irregular eutectic structure (with branches) appears at low growth rates. The regular lamellar eutectic structure is observed at middle growth rates. The regular rod-like eutectic structure exists exclusively in the stripes at some elevated growth rates. A new thermodynamic criterion is recommended. It suggests that this eutectic regular structure is the winner in a morphological competition for which the minimum entropy production is lower. A competition between the regular rod-like and the regular lamellar eutectic growth is described by means of the proposed criterion. The formation of branches within irregular eutectic structure is referred to the state of marginal stability. A continuous transitions from the marginal stability to the stationary state are confirmed by the continuous transformations of the irregular eutectic structure into the regular one.

Keywords: Eutectic structure selection, (Zn) – single crystal, Branching phenomenon

1. Introduction

The (Zn) – hexagonal single crystal can be produced by the *Bridgman* method with appropriately imposed both a constant growth rate, v , and a constant positive thermal gradient, G , [1]. Usually, the stationary state is ensured for the single crystal formation by the directional solidification. The investigated zinc alloys contain a small additions of titanium and cooper. Therefore, some eutectic stripes are expected to appear in the (Zn) - single crystal morphology, [1]. Moreover, the phenomenon of

the Ti - solute segregation should appear in the single crystal bar. In fact, the segregation has already been revealed and described for the inter-stripes region, [2]. The description was possible due to an equation developed generally for some hypo-eutectic alloys, [3]. The mentioned equation is associated with the solute segregation and redistribution after back-diffusion.

The reinforcement of the (Zn) – single crystal as a whole depends on the stripes width and on the type of eutectic structure in the stripes. The origin of the stripes appearance results from the

nature of the Zn-Ti phase diagram in which the eutectic point is situated near the Zn, [4].

The eutectic stripes are localized periodically along the (Zn) – single crystal bar, Fig. 1a. The structure transformations in the stripes occur in terms of the applied growth rate, v , [1].

Since the back-diffusion intensity depends on the crystal growth rate, v , [5], the small adjustments of the stripe width are possible through the growth rate choice. It occurs, because the crystal growth rate, v , decides on the creation of an additional precipitate, that is the non-equilibrium eutectic precipitate, $i_N(v)$, [5]. First of all, the stripe width depends on the nominal titanium concentration, N_0 , in an alloy subjected to the unidirectional solidification. The choice of the N_0 - nominal solute content decides on the appearing of the equilibrium eutectic precipitate, $i_D(N_0)$, [5], and in the consequence on the stripe width. The higher is the solute concentration in a hypo-eutectic alloy the bigger is an amount of the equilibrium eutectic precipitate, i_D . It becomes obvious, that the (Zn) – single crystal strengthening can be controlled experimentally not only by an application of the proper crystal growth rate, v , to the *Bridgman* system but additionally, by the selection of the N_0 - nominal titanium concentration in the studied Zn-Ti-Cu alloy as well.

In the current model, some transitions from one to another eutectic structure in the stripes will be confirmed theoretically with the use of a new thermodynamic criterion which is recommended. The criterion suggests that this eutectic regular structure, lamellar or rod-like, is the winner in a morphological competition for which the minimum entropy production is localized lower. Additionally, a concept of marginal stability will be introduced to justify the appearance of a branching phenomenon in the irregular eutectic structure.

2. Experiment

The growth of the (Zn) – single crystal was performed by the *Bridgman* system equipped with the moving temperature filed. The applied growth rates were situated within the range: $3 < v \leq 16$ [mm/h]. The thermal gradient created at the solid / liquid (s/l) interface of the growing single crystal was about: $G \approx 80$ [K/cm]. A graphite crucible was used in the experiments. Additionally, a protective argon atmosphere was applied to the *Bridgman* system furnace. Some ingots of the ZnTi0.01, ZnTi0.02 and ZnTi0.1[wt %] alloys, were prepared as a charge to the *Bridgman* system. The size of the produced (Zn) – single crystals was 26x6x120 [mm].

The studied (Zn) – single crystal was doped by an amount of copper, (0.1 or 0.15 [wt %]). The addition of copper modifies the specific surface free energy of the s/l interface. In the consequence, some higher crystal growth rates (up to 16 [mm/h]) could be imposed in the experiment.

Copper does not form any inter-metallic compound with the zinc but is localized in the (Zn) - zinc / titanium solid solution. The titanium forms the *faceted* inter-metallic compound with the zinc, Zn₁₆Ti, Fig. 1b.

When a given nominal solute concentration is fixed, a control of the stripes width is possible by the selection of the growth rate, v , only. It is obvious, because the imposed growth rate, v , decides on the value of the back-diffusion parameter, $\alpha(v)$, during solidification, [5] and finally on the amount of the non-equilibrium eutectic precipitate, i_N , as mentioned. The stripes appear in the (Zn) – single crystal in a cyclical manner with a constant inter-stripe spacing, Fig. 1a.

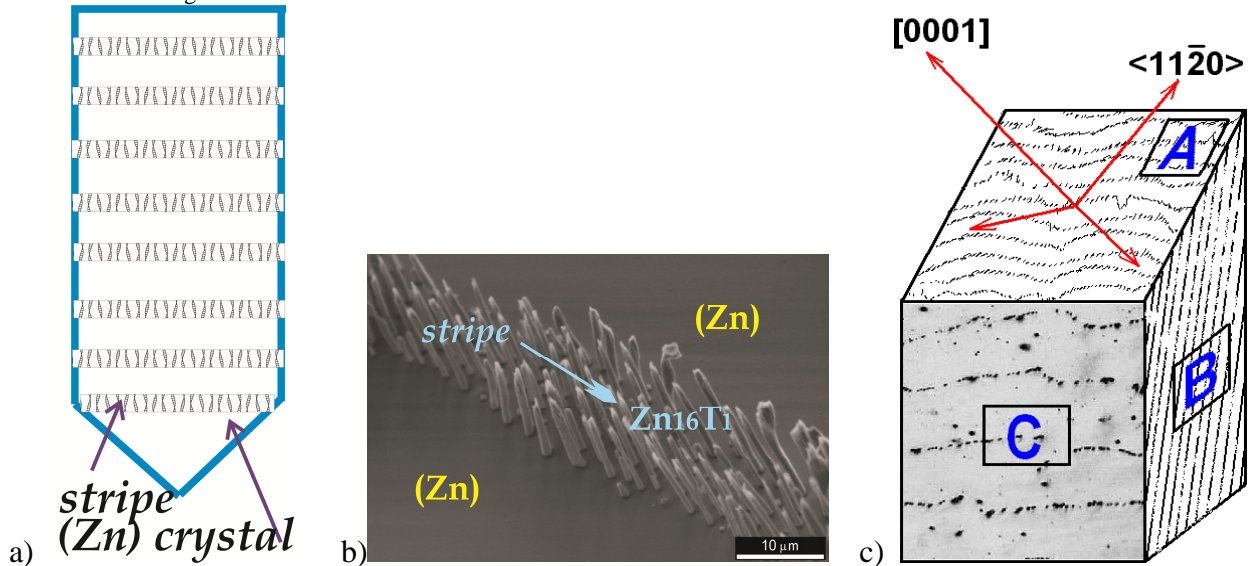


Fig. 1. (Zn) single crystal, a) stripes localized periodically in the (Zn) – single crystal along its axis (scheme), b) regular rod-like morphology of the stripe, $(Zn) \equiv \alpha$, c) crystallographic orientation of the Zn₁₆Ti – eutectic phase and localization of stripes within the single crystal

The regular eutectic morphology appears in the stripes in the following manner:

- 1) for the $0 < v < v_1$ growth rates range, the areas of regular L-shape rods exist inside a generally irregular rod-like eutectic morphology,
- 2) for the $v_1 < v < v_1'$ growth rates range, the transitions from irregular rods into regular rods (disappearing of branches) and next into the regular lamellae occur; so, rods and lamellae co-exist in the stripes morphology,
- 3) for the $v_1' < v < v_2$ growth rates range, the regular lamellae are the exclusive form,
- 4) for the $v_2 < v < v_3$ growth rates range, regular rods appear in the stripes, only.

The threshold growth rates are: $v_1 = 5$, $v_1' = 5.8$, $v_2 = 10$ and $v_3 = 16$ [mm/h].

3. Thermodynamics of the stripe morphology formation

The eutectic morphology formation in the stripes is justified thermodynamically.

First of all, a steady-state growth is ensured because the constant crystal growth rate, v , and a constant positive thermal gradient, G , are applied during solidification in the *Bridgman* system.

Generally, two eutectic morphologies are distinguished:

- a) regular morphology defined by only one selected inter-phase spacing when a given growth rate is applied; the spacing corresponds to the minimum entropy production in the envisaged system,
- b) irregular morphology in which the perturbation waves appear at the s/l interface of the *non-faceted* phase; consequentially a branching phenomenon occurs, Fig. 2.

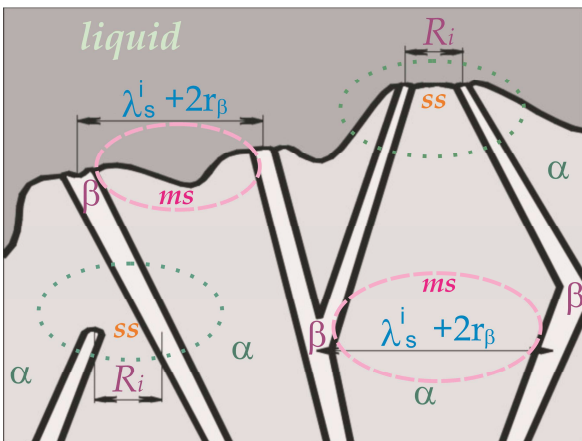


Fig. 2. Generally irregular eutectic structure with some areas of the regular eutectic structure (the scheme reproduced after, [6])

When the perturbation evinces its maximal wavelength then the *ms* - marginal stability is reached in this area, as assumed in the current model.

Next, the perturbation wave decays and this local s/l interface tends to have a parabolic shape, typical for the structure formed under the *ss* - stationary state. Finally, this *ms* - maximally irregular area of structure (with the branch birth) becomes the *SS* - regular structure situated inside the generally irregular eutectic structure, Fig. 2.

λ_s^i - perturbation maximal wavelength which can appear at the s/l interface of the α - *non-faceted* eutectic phase, r_β - rod radius of the $\beta = \text{Zn}_{16}\text{Ti}$ - *faceted* phase, R_i - inter-rod spacing for the regular eutectic structure, *ss* - area of the structure formation (regular one) in the stationary state, *ms* - area of the structure formation with the presence of a maximal perturbation of the s/l interface of the *non-faceted* phase and the birth of the *faceted* phase branch.

3.1. Crystal growth in the stationary state

Two types of the regular eutectic morphology appear in the stripes: rod-like and lamellar one. It involves the calculation of the entropy production for both mentioned structures formation. The general definition of the entropy production per unit time, P_s^D , (connected with the mass transfer, only) is:

$$P_s^D = \int_V \sigma dV \quad S = R, L \quad (1)$$

V - volume selected in the system (inside the V , all essential fluxes must occur, [7]);

σ - entropy production per unit time and unit volume, $[\text{mole fr.}^2 / (\text{m}^3 \text{s})]$, calculated for a constant temperature, ($T_E - \Delta T(v)$), of the s/l interface of the growing eutectic stripe;

where ΔT is the s/l interface undercooling;

subscript: $S = R, L$, is: R - for rod-like, L - for lamellar structure formation.

$$\sigma = R^* \varepsilon C^{-1} (1-C)^{-1} D \nabla^2 C \quad (1a)$$

R^* - gas constant, $[J / (\text{mole } K)]$;

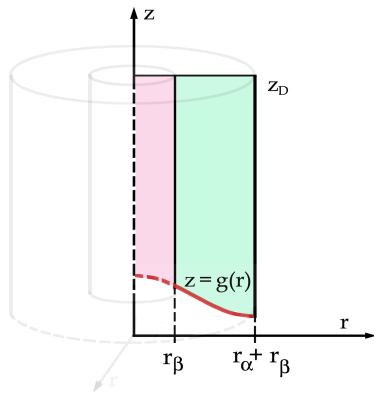
ε - thermodynamic factor, [dimensionless];

C - solute content in the liquid, [at.%];

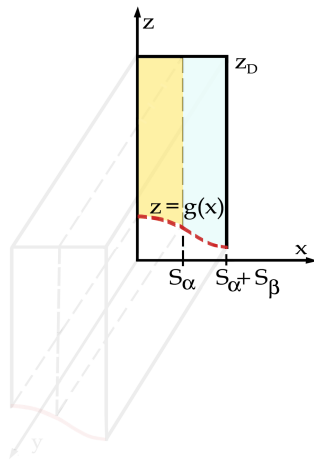
D - diffusion coefficient, $[\text{m}^2 / \text{s}]$.

The V - volume, (adequate for integration, Eq. (1)), is determined in Fig. 3.

The s/l interface curvature, $z = g(r)$; $z = g(x)$, has a crucial effect on the concentration field in the liquid, [8]. Therefore, the s/l interface shape is analyzed in the current description, Fig. 3.



a)



b)

Fig. 3. The V - volume, applied in calculation of the entropy production per unit time, Eq. (1); a/ for the rod-like regular structure, where $z = g(r)$ - function describes the s/l interface curvature; b/ for the regular lamellar structure, where $z = g(x)$ - function describes the s/l interface curvature; z_D is a thickness of the diffusion boundary layer at the s/l interface, [m]

$$R_i = 2(r_\beta + r_\alpha) \quad \lambda_i = 2(S_\alpha + S_\beta) \quad (1b)$$

Eq. (1a) contains the terms: $D\nabla^2 C(x, z)$ for the regular lamellae or $D\nabla^2 C(r, z)$ for the regular rods growth, respectively. Therefore, Eq. (1) requires to consider, at least, the simple solution for diffusion equation with the cosine series common for both lamellae, [9]. However, a more realistic solution for diffusion equation with the cosine series treated separately for each lamella, [10], should be applied.

In this case, the diffusion equation for the stationary regular eutectic growth: $D\nabla^2 C(x, z) + v \partial C(x, z) / \partial z = 0$, yields the following solution:

a) for the α - eutectic lamella formation (the Zn) - non-faceted phase in the Zn - Ti system,

$$\delta C(x, z) = \sum_{n=1}^{\infty} A_{2n-1} \cos\left(\frac{(2n-1)\pi x}{2S_\alpha}\right) \exp\left(-\frac{(2n-1)\pi}{2S_\alpha} z\right) \quad (2)$$

$$A_{2n-1} = -\frac{4}{(2n-1)\pi} \int_0^{S_\alpha} f_\alpha(x) \cos\left(\frac{(2n-1)\pi x}{2S_\alpha}\right) dx \quad n=1, 2, \dots \quad (2a)$$

b) for the β - eutectic lamella formation (the Zn₁₆Ti) - faceted phase in the Zn - Ti system,

$$\delta C(x, z) = \sum_{n=1}^{\infty} B_{2n-1} \cos\left(\frac{(2n-1)\pi(x - S_\alpha + S_\beta)}{2S_\beta}\right) \exp\left(-\frac{(2n-1)\pi}{2S_\beta} z\right)$$

$$B_{2n-1} = -\frac{4}{(2n-1)\pi} \int_{S_\alpha - S_\beta}^{S_\alpha} f_\beta(x) \cos\left(\frac{(2n-1)\pi(x - S_\alpha + S_\beta)}{2S_\beta}\right) dx$$

(3a) where, f_j - function applied to the boundary condition,

[at.%], ($j = \alpha, \beta$), respectively; x, z - geometrical coordinates,

[m].

The above solutions, Eq. (2), Eq. (3) satisfy the local mass balance, Eq. (4), provided the d - faceted phase protrusion, is taken into account, Fig. 4.

$$\int_0^{S_\alpha} \delta C(x, 0) dx + \int_{S_\alpha}^{S_\alpha + S_\beta} \delta C(x, d) dx = 0 \quad (4)$$

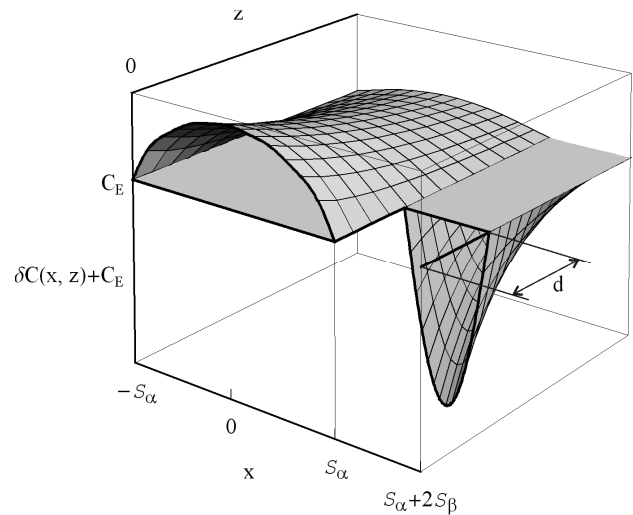


Fig. 4. Visualization of the faceted phase protrusion, d ; the value of the d - parameter results from the local mass balance calculation, Eq. (4), performed for the solute concentration micro-

field in the liquid, localized in front of the $(\alpha + \beta)$ eutectic lamellae

The presence of the d - faceted phase protrusion, predicted theoretically, Fig. 4, has been revealed in the stripe morphology, as shown in Fig. 5.

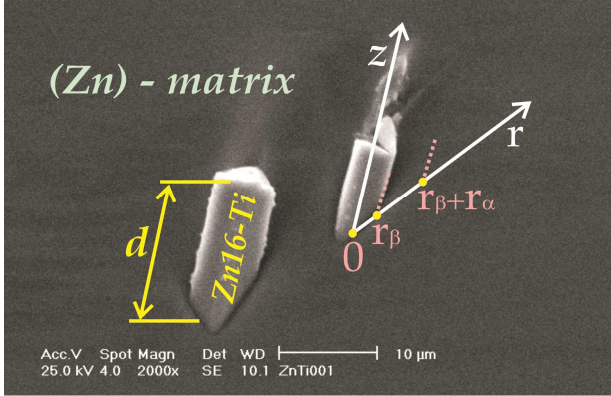


Fig. 5. The $Zn_{16}Ti$ phase protrusion, d , revealed in the stripes; the (r, z) - coordinate system is attached to the s/l interface advancing in the z - direction with the velocity, v , at stationary state; the system localizes the Ti - solute concentration micro-field in front of the $(\alpha + \beta)$ - eutectic structure

Additionally, some values of the specific surface free energies, $\sigma_{Zn_{16}Ti}^L(v)$; $\sigma_{(Zn)}^L(v)$; $\sigma_{(Zn)-Zn_{16}Ti}^L(v)$, Fig. 6, are to be introduced into the entropy production calculation based on Eq. (5), Eq. (6). The energies must satisfy the mechanical equilibrium considered at the triple point of the s/l interface, (vectors parallelogram), for each of the crystal growth rate, v , [11].

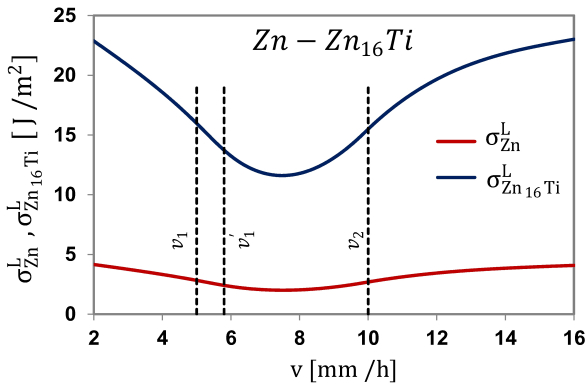


Fig. 6. Changes of the specific surface free energy, $\sigma_{(Zn)}^L$, and inter-phase boundary free energy, $\sigma_{(Zn)-Zn_{16}Ti}^L$ in terms of the growth rate, v ; their values vary with the eutectic phases anisotropy (with a rotation of the crystallographic orientation of the both eutectic phases)

The final definition of the entropy production per unit time is as follows:

$$P_R^D = V_1 v (r_\beta + r_\alpha)^{-1} + V_2 v (r_\beta + r_\alpha)^{-2} + V_3 v^2 + V_4 v^2 (r_\beta + r_\alpha) + V_5 v^3 (r_\beta + r_\alpha)^2 \quad (5)$$

$$P_L^D = W_1 v (S_\alpha + S_\beta)^{-1} + W_2 v (S_\alpha + S_\beta)^{-2} + W_3 v^2 + W_4 v^2 (S_\alpha + S_\beta) + W_5 v^3 (S_\alpha + S_\beta)^2 \quad (6)$$

$V_n; W_n$ $n=1, \dots, 5$ coefficients contain material parameters, [12]; $r_j; j = \beta, \alpha; S_j; j = \alpha, \beta$ - parameters describe the geometry of rod-like (R) and lamellar (L) eutectic structure within the V - volume, as shown in Fig. 3.

The regular eutectic structure formation is observed when the solidification occurs in the stationary state. The stationary state is well described by the criterion of minimum entropy production, [13], [14]. The criterion ($\partial P^D / \partial r|_v = 0$; or $\partial P^D / \partial \lambda|_v = 0$) selects the unique inter-phase spacing, R_r or λ_r , for the regular eutectic structure. Its application to Eq. (5) and Eq. (6) yields the so-called growth laws:

a) growth law for the regular rod-like structure formation,

$$2 V_5 v^2 (r_\beta + r_\alpha)^4 + V_4 v (r_\beta + r_\alpha)^3 - V_1 (r_\beta + r_\alpha) = 2 V_2 \quad (7)$$

b) the growth law for the regular lamellar structure formation,

$$2 W_5 v^2 (S_\alpha + S_\beta)^4 + W_4 v (S_\alpha + S_\beta)^3 - W_1 (S_\alpha + S_\beta) = 2 W_2 \quad (8)$$

The minimization of Eq. (5) and Eq. (6) allows for describing the competition between both regular structures (lamellar and rod-like) formation in the stripes. This structure (lamellar or rod-like) is the winner in a thermodynamic competition for which the minimum entropy production is situated lower as assumed in the current model. The application of the suggested criterion to the description of the thermodynamic competition in the stripes is shown in Fig. 7.

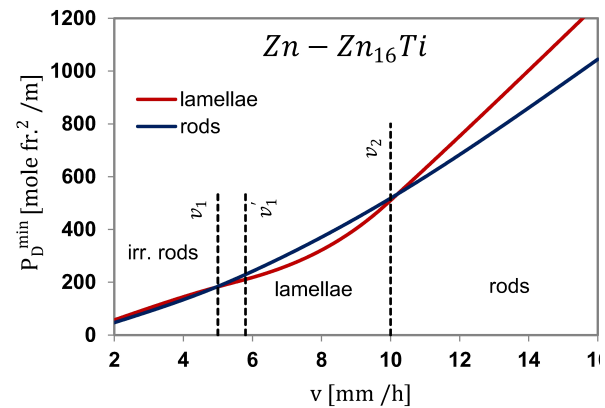


Fig. 7. Theoretical visualization of the thermodynamic competition between regular structures formation in the stripes strengthening the (Zn) - single crystal; P_D^{\min} is the minimal entropy production calculated on the basis of Eq. (5) and Eq. (6)

The minimal entropy production is situated lower either for the regular lamellae or the regular rods formation. This localization depends on the range of growth rates, Fig. 7.

The analysis, (Fig. 7), does not describe the branching phenomenon observed over the growth rates range, $0 < v \leq v_1$, when irregular eutectic structure is formed. Moreover, this study does not explain how the decay of branches occurs over the range, $v_1 < v \leq v_1'$, when the irregular rod-like structure transforms into regular lamellar eutectic structure.

When the branching phenomenon occurs, the criterion of minimum entropy production is not sufficient to describe the structure formation. The current model suggests to introduce, additionally, the concept of marginal stability as shown in Fig. 2.

3.2. Crystal growth at the marginal stability

In the case of the irregular eutectic structure formation in the stripes, ($0 < v \leq v_1$), some areas which can be referred to the marginal stability are found, Fig. 8. In fact, a freezing of the stripes s/l interface allowed for showing maximal perturbation of the s/l interface of the *non-faceted* (Zn) – phase, Fig. 8.

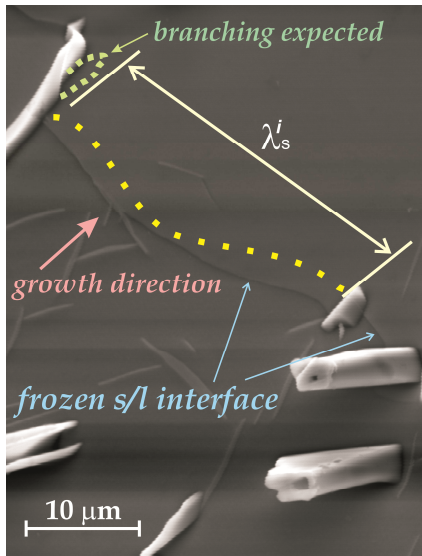


Fig. 8. The maximal wavelength of the s/l interface perturbation visible in the stripe area of the extremely irregular morphology; the dotted line is juxtaposed to show more visibly the undulating shape of the s/l interface

At the same time, the branching phenomenon is expected in the area of maximal perturbation, Fig. 8. The just born branch tends to minimize the distance between two neighboring rods. Eventually, this distance will reach the R_i - value which corresponds well to the stationary state, Fig. 9. At the stationary state the branch ends to grow.

It can be concluded that the stationary state plays the role of an attractor in the envisaged system, Fig. 10.

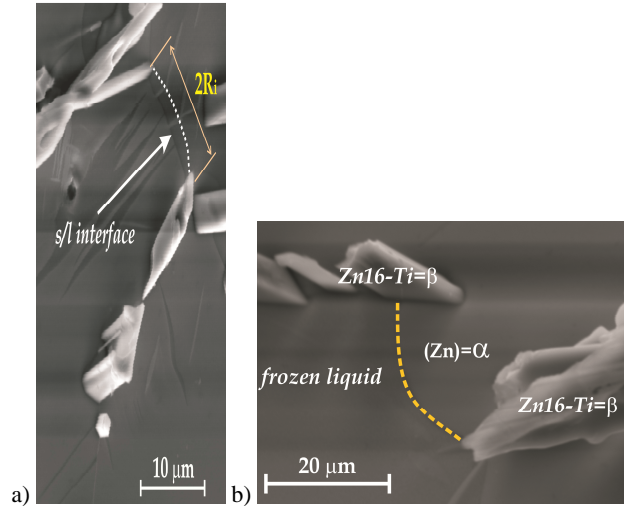


Fig. 9. Rod-like irregular eutectic structure revealed in the stripe; a) the minimal R_i - inter-rod spacing distinguished in the generally irregular structure; the dotted line is added to show the parabolic shape of the s/l interface, (shape characteristic for the regular morphology, [15]); b) the minimal inter-rod spacing revealed in the stripe structure; the dashed line is superposed over the s/l interface to emphasize its characteristic parabolic shape

The maximal wavelength, λ_s^i , Fig. 8, can be defined as:

$$\lambda_s^i = 2\pi \left(\Gamma_{(Zn)} / (G - m_{(Zn)} G_C) \right) \quad (9)$$

$\Gamma_{(Zn)}$ - Gibbs-Thomson capillarity parameter; $m_{(Zn)}$ - slope of the liquidusline for the (Zn) – phase; G_C - solute concentration gradient at the s/l interface of the (Zn) – eutectic phase which appears in a given stripe.

Some remaining parts of stripe morphology are in the mid-states, that is, between the completion of a given branch growth, Fig. 9, and the beginning of a given branch growth, Fig. 8. Thermodynamically, these parts of morphology are in the mid-states situated between A - point (stationary state) and B – point (marginal stability state), Fig. 10.

Eventually, it can be concluded that the stripes morphology formation occurs in a cyclical manner.

The paraboloid, Fig. 10b, is cut by the $G_o = const.$ - plane, to show the oscillation between, the A and B points situated on the local parabola, as explained in Fig. 10a. The G_o - thermal gradient is associated with the v_o - crystal growth rate which involves the R_{io} - spacing appearance and with the v_o' - crystal growth rate which yields a perturbation wave creation (with the $\lambda_{s_o}^i$ wavelength), $v_o > v_o'$, because the appearance of the perturbation makes the *non-faceted* phase growth a little sluggish.

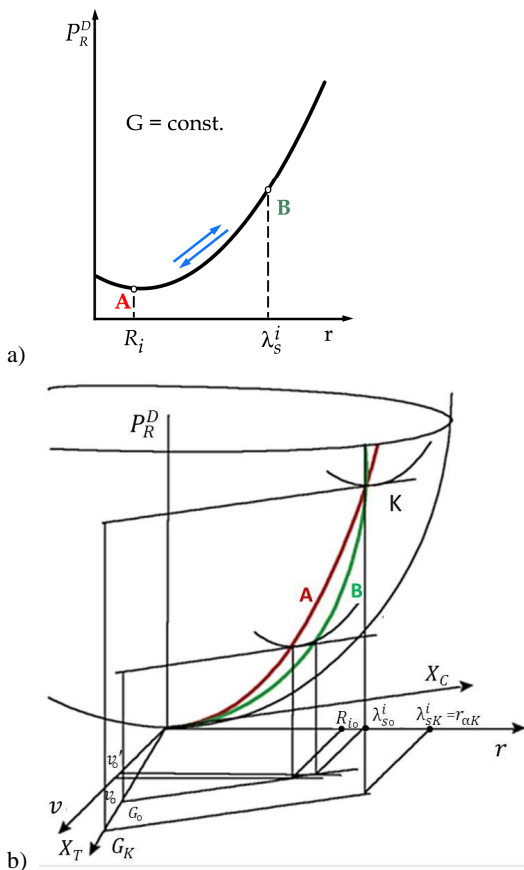


Fig. 10. A cyclical manner of the irregular eutectic structure formation in the stripes; a) an oscillation between the *A* - stationary state, and the *B* - marginal stability state, shown on the entropy production parabola which is drawn schematically for a given thermal gradient, *G*, b) a paraboloid of the entropy production (the same paraboloid is assumed to be valid: *A*) for the (X_T, X_C) coordinate system and *B*) for the (v, r) coordinate system), $X_T \equiv G$; X_T - thermodynamic force associated with the heat transfer, $X_C \equiv G_C$; X_C - thermodynamic force associated with the mass transport (thermo-diffusion)); the red trajectory contains the local minima of the paraboloid, and the green trajectory shows the localization of marginal stability states on the same paraboloid

The paraboloid of the entropy production, $P_R^D(r, v)$, is cut by the *K* - plane to show the vanishing of the cyclical manner of the structure formation at the G_K - critical thermal gradient. At the critical thermal gradient the branching phenomenon is not possible. Consequentially, the marginal stability cannot appear in some areas of structure. The analogous situation is created at the small growth rates, when, $v \rightarrow 0$, Fig. 10b. Then, the irregular eutectic structure transforms perfectly into the regular structure as confirmed experimentally for the Al-Si system, [16].

4. Concluding remarks

Two thermodynamic states are distinguished for the eutectic structure formation in the stripes appearing periodically in the (Zn) - single crystal:

- the stationary state defined by the minimum entropy production referred to the regular structure appearance,
- the marginal stability state defined by the maximal wavelength of perturbation referred to the birth of branches in the irregular structure.

Some structural transformations are observed in the stripes strengthening the (Zn) - single crystal:

- regular lamellae transform into regular rods, at the v_2 - threshold growth rate,
- irregular rods transform into regular rods and at the same time transition from the regular rods to the regular lamellae occurs, over the $v_1 \div v_1'$ range of the growth rates.

The regular structure transforms into another regular structure at the threshold growth rate, immediately, (for example: v_2 in Fig. 7).

However, the irregular into a regular structure transition requires the certain range of growth rates to be applied, experimentally, $(v_1 \div v_1')$ in Fig. 7).

The range of growth rates was also necessary to be applied in the case of the Al-Si irregular lamellar into the regular rod-like structure transition, [17].

The ranges of growth rate (associated with the structural transitions) are required by the progressive vanishing of branches, in both mentioned situations.

When the irregular into the regular structure transition occurs, it means that the system recedes consequently from the marginal stability to achieve the stationary state, exclusively, as observed experimentally in the stripes for, the v_1' - growth rate.

This phenomenon confirms that the stationary state plays the role of an attractor for the investigated system.

The recommended thermodynamic criterion connected to the structural competitions observed in the stripes has been successfully verified, Fig. 7.

According to the verified criterion the system selects this regular eutectic structure: lamellar or rod-like, for which the minimum entropy production is situated lower.

The theoretical predictions, Fig. 7, confirm that the rod-like regular structure is formed twice, over the $0 < v < v_1$ (locally) and $v_2 < v < v_3$ rate ranges.

So, the predictions are in good agreement with the experimental observations of the stripes morphology.

However, the above confrontation is possible provided the surface energies are treated as the anisotropic energies, Fig. 6.

The use of both

- criterion of minimum entropy production
- concept of marginal stability

allows for explaining the cyclical manner of the irregular eutectic morphologies formation in the strengthening stripes, as shown in Fig. 10a, $(A \Leftrightarrow B)$. It occurs, when the crystal growth rates satisfy the following formula, $0 < v < v_1$.

Acknowledgements

In particular, we want to express our sincere gratitude to Dr hab. inż. G. Boczek. Without his constant support and great patience with experimental observations this paper would never have been written. The (Zn) - single crystals were produced at the Faculty of Non-Ferrous Metals of the AGH University of Science and Technology, Kraków.

References

- [1] Boczek, G., Mikułowski, B. & Wołczyński, W. (2010). Oscillatory Structure of the Zn-Cu-Ti Single Crystals. *Materials Science Forum*. 649, 113-118.
- [2] Wołczyński, W. (2013). Thermodynamic Pattern Selection in the Stripes Generated Periodically during the (Zn) – Single Crystal Growth. *Archives of Metallurgy and Materials*. 58, 309-313.
- [3] Wołczyński, W., Krajewski, W., Ebner, R. & Kloch, J. (2002). The Use of Equilibrium Phase Diagram for the Calculation of Non-Equilibrium Precipitates in Dendritic Solidification. Theory. *Calphad*. 25, 401-408.
- [4] Wołczyński, W. (2000). Back-Diffusion Phenomenon during the Crystal Growth by the Bridgman Method. In Szmyd, J. & Suzuki K. (Eds.), *Modelling of Transport Phenomena in Crystal Growth* (pp. 19-59). WIT Press, Southampton–Boston.
- [5] Murray, J. (1987). Phase Diagram of Binary Titanium Alloys. In Massalski T. (Ed.), *Binary Alloy Phase Diagrams* (pp. 336-339) ASM International, Metals Park, Ohio.
- [6] Fisher, D. J. & Kurz, W. (1980). A Theory of Branching Limited Growth of Irregular Eutectics. *Acta Metallurgica* 28, 777-794.
- [7] Glansdorff, P. & Prigogine, I. *Thermodynamic Theory of Structure, Stability and Fluctuations*. Wiley–Interscience, John Wiley & Sons, London–New York–Sydney–Toronto.
- [8] Colin, M., Lesoult, G. & Turpin, M. (1975). Influence de la Forme de l'Interface Liquid/Solid sur la Diffusion Chimique pendant une Solidification Eutectique Lamellaire. *Journal of Crystal Growth*. 28, 103-108.
- [9] Jackson, K.A. & Hunt, J. D. (1966). Lamellar and Rod Eutectic Growth. *Transactions of the Metallurgical Society of the AIME*. 236. 1129-1142.
- [10] Wołczyński, W. (2007). Concentration Micro-Field for Lamellar Eutectic Growth. *Defect and Diffusion Forum*. 272, 123-138.
- [11] Wołczyński, W. (1990). Role of Physical Factors in Solid-Liquid Interface Formation during Oriented Eutectic Growth. *Crystal Research and Technology*. 25, 1303-1309.
- [12] Wołczyński, W. & Billia, B. (1996). Influence of Control and Material Parameters on Regular Eutectic Growth and Inter-Lamellar Spacing Selection. *Materials Science Forum*. 215/216, 313-322.
- [13] Kjelstrup, S. & Bedeaux, D. (2008). *Non-Equilibrium Thermodynamics of Heterogeneous Systems*. In Rasetti M. (Ed.). World Scientific Publishing Co. Ltd., New Jersey–London–Singapore–Beijing–Shanghai–Hong Kong–Taipei–Chennai.
- [14] Wołczyński, W. (1989). Lamellar Eutectic Growth at Minimum Entropy Production. *Crystal Research and Technology*. 24, 1121-1127.
- [15] Wołczyński, W. (1992). Parabolic Approximation to the Shape of Oriented Eutectic Interface. *Crystal Research and Technology*. 27, 195-200.
- [16] Major, J.F. & Rutter, J.W. (1989). Effect of Strontium and Phosphorus on Solid / Liquid Interface of Al-Si Eutectic. *Materials Science and Technology*. 5, 645-656.
- [17] Cupryś, R. & Wołczyński, W. (1999). Influence of the Growth Parameters of an Eutectic onto the Transition of Flake into Fibre. Structure in Al-Si Alloy. *Acta Metallurgica Slovaca*. 5, 359-364.